transplantology

MDPI

Article

Slice of Life: Porcine Kidney Slices for Testing Antifibrotic Drugs in a Transplant Setting

L. Leonie van Leeuwen [1,*] , **Mitchel J. R. Ruigrok** [2], **Henri G. D. Leuvenink** [1] **and Peter Olinga** [2]

[1]   Department of Surgery, University Medical Center Groningen, University of Groningen, Hanzeplein 1,
     9713 GZ Groningen, The Netherlands
[2]   Department of Pharmaceutical Technology and Biopharmacy, Groningen Research Institute of Pharmacy,
     University of Groningen, Antonius Deusinglaan 1, 9713 AV Groningen, The Netherlands
*   Correspondence: l.l.van.leeuwen@umcg.nl; Tel.: +31-6-2476-2959

Abstract: Circulatory death donor (DCD) kidneys are increasingly used to enlarge the donor pool. These kidneys undergo ischemia-reperfusion injury, frequently leading to renal fibrosis. Transforming growth factor beta 1 (TGF-β1) and matrix metalloproteases have been identified as central mediators of fibrosis and inhibition of these targets could attenuate fibrosis. We studied whether galunisertib, doxycycline, taurine, and febuxostat alleviated fibrosis in precision-cut kidney slices (PCKS). PCKS were prepared from porcine kidneys that were exposed to 30 min of warm ischemia followed by 3 h of oxygenated hypothermic machine perfusion. We subsequently incubated PCKS for 48 h at 37 °C with the described compounds. To further elucidate the antifibrotic effects of galunisertib, we cultured PCKS with TGF-β1. We first screened the effects of the compounds without TGF-β1. Most significant effects were observed for galunisertib which lowered the expression of *ACTA2*, *TGFB1*, *FN2*, and *SERPINE1*. We then investigated the effects of galunisertib in fibrotic PCKS incubated with TGF-β1. TGF-β1 significantly increased expression of *TGFB1*, *FN1*, *SERPINE1*, and *SERPINH1*. Galunisertib, however, attenuated the expression of all fibrosis-related genes. Galunisertib appears to be a promising antifibrotic compound requiring further research in a preclinical model and may ultimately be administered during machine perfusion as an antifibrotic treatment in a transplant setting.

Keywords: donation after circulatory death; kidney transplantation; ischemia-reperfusion injury; fibrosis; normothermic machine perfusion; precision-cut kidney slices

1. Introduction

Chronic kidney disease is currently prevalent in 11% of the world's population and this number is still rising. It is characterized by a gradual loss of renal function due to interstitial fibrosis, often requiring a kidney transplant for survival [1,2]. As waiting lists keep growing, the need for additional donor kidneys is crucial. Consequently, suboptimal kidneys such as circulatory death donor (DCD) kidneys are increasingly used to enlarge the donor pool [3–5]. Unfortunately, these kidneys are deprived of nutrients and are subjected to the re-introduction of oxygen—possibly leading to ischemia-reperfusion injury, delayed graft function, interstitial fibrosis, and renal failure [6,7].

The most common cause for kidney allograft failure is chronic allograft nephropathy which is characterized by interstitial fibrosis and tubular atrophy [8]. Interstitial fibrosis is a common pathological process characterized by an imbalanced extracellular matrix (ECM). Multiple pathways have been shown to play a role in the formation and progression of interstitial fibrosis by inducing inflammation, endothelial-to-mesenchymal transition, epithelial-mesenchymal transition (EMT), activating fibroblasts, and ECM formation [9–12]. One of the most important cytokines involved in fibrogenesis is transforming growth factor beta 1 (TGF-β1) [13,14]. TGF-β1 primarily causes tissue scarring by activating its

downstream small mother against the decapentaplegic (SMAD) signaling pathway [15]. Inhibiting TGF-β1 has shown significant reductions in renal fibrosis formation in rat and mice models yet this has not yet been explored in a transplant setting [16]. While the accumulation of ECM proteins certainly play a role in fibrosis and chronic rejection, recent studies show that excessive degradation of the ECM also plays a pathophysiological role [17–19]. One of the proteases responsible for this degradation—matrix metalloprotease 9 (MMP9)—is a key protein in the development of kidney fibrosis [20,21]. Furthermore, studies show that MMP2 and 9 contribute to fibrosis formation by promoting EMT and the activation of fibroblasts [16]. Therefore, TGF-β1 and MMP2/9 could be promising drug targets to attenuate fibrosis caused by transplant-related injury.

Galunisertib, taurine, febuxostat, and doxycycline represent compounds that could potentially attenuate renal fibrosis by modulating TGF-β1 signaling and MMP2/9 activity in a transplant setting. Galunisertib—originally developed as anti-cancer treatment—is an inhibitor of the TGF-β1 receptor kinase which lowers the phosphorylation of SMAD2/3 [22]. It has already been shown that galunisertib has antifibrotic potency in liver and renal fibrosis [23,24]. Taurine—an organic acid, and a derivative of the amino acid cysteine—is another compound that modulates TGF-β1 signaling. It significantly reduces TGF-β1 expression via inhibition of the MAPK pathway which plays an important role in TGF-β1 production in cells [25]. Furthermore, studies have shown that taurine has antioxidative, antiapoptotic, and anti-inflammatory capacities, and protective effects against renal interstitial fibrosis in rats [25–27]. Febuxostat—commonly used to treat gout—also modulates TGF-β1 signaling by activating the bone morphogenetic protein-7 (BMP-7) pathway. BMP-7 is a naturally existing inhibitor of the TGF-β1-dependent, pro-fibrotic pathway and protects the kidney against fibrosis, making it a promising drug target [28]. Finally, doxycycline—a tetracycline-class antibiotic—is known for its inhibitory action on MMP activity. Research has indicated that it has protective effects during renal ischemia-reperfusion injury and against fibrosis by attenuating MMP2 and 9 activity and TGF-β expression [29–33].

The implementation of renal normothermic machine perfusion (NMP) provides a unique avenue for treating isolated organs in an ex vivo manner. During NMP, kidneys are rewarmed to normothermic temperatures (35–37 °C) to restore metabolism and allow for functional evaluation of the graft [34–36]. Additionally, pharmacologically active substances, such as the ones described above, can be administrated during NMP to repair suboptimal donor kidneys [37]. The main advantage of treating an isolated organ is that systemic effects are avoided and, therefore, more potent drugs can be used.

Before administrating these drugs in a (experimental) perfusion setup, precision-cut kidney slices (PCKS) could be used as an intermediate experimental model to bridge the gap between in vitro and in vivo approaches [38]. PCKS is a novel technique to study multicellular processes as the organ architecture is maintained [39,40]. Thousands of PCKS can be obtained from just one kidney. This allows for testing of compounds using slices from the same biological source, thereby reducing biological variation. PCKS have been proven successful in investigating fibrotic processes and antifibrotic compounds in renal tissue [24,39,41]. By exposing kidneys to warm ischemia, and thus mimicking donation after circulatory death before slicing, it becomes possible to test compounds in a DCD-PCKS model [38].

Our aim was to test the antifibrotic potency of galunisertib, doxycycline, taurine, and febuxostat in a porcine DCD-PCKS model. PCKS were prepared from porcine kidneys that were exposed to 30 min of warm ischemia followed by 3 h of oxygenated hypothermic machine perfusion. We subsequently incubated PCKS for 48 h at 37 °C with the described compounds. To further elucidate the antifibrotic effects of galunisertib in a fibrotic environment, we cultured PCKS with TGF-β1.

2. Materials and Methods

2.1. Animal Model

All experiments were carried out with porcine kidneys. These kidneys were retrieved from a local slaughterhouse after a highly standardized slaughtering process. The pigs were anaesthetized using an electric shock followed by exsanguination. The kidney of choice was determined based on macroscopic morphology (e.g., undamaged condition, color, shape, arterial branching). All kidneys were flushed with 180 mL of ice cold 0.9% saline solution (Fresenius Kabi, Sèvres, France) after 30 min of warm ischemia time. This way each kidney underwent warm ischemic injury.

2.2. Hypothermic Machine Perfusion

As hypothermic machine perfusion (HMP) is standard clinical care for deceased donor kidneys in the Netherlands, kidneys were preserved and transported using HMP. Kidneys were surgically prepared and connected to the Kidney Assist Portable (XVIVO, Gothenburg, Sweden) perfusion machine. HMP was performed for 3 h at a set mean arterial pressure of 25 mmHg. A quantity of 230 mL of oxygenated (100 mL/min) University of Wisconsin (UW) perfusion solution (Bridge to Life Ltd., London, UK) was used at 3–5 °C.

2.3. Precision-Cut Kidney Slices

After HMP, the kidneys were immediately flushed with 120 mL of ice cold 0.9% saline solution. Using a 10 mm blade, the renal capsule was carefully removed. Cores were drilled from the cortex with a 6 mm biopsy punch and stored in ice cold UW cold storage solution.

PCKS were obtained using the Krumdieck tissue slicer (Alabama Research and Development, Munford, TN, USA). The Krumdieck slicer was assembled and filled with Krebs-Henseleit buffer (25 mM NaHCO$_3$, B. Braun, Melsungen, Germany), 25 mM D-glucose (Merck, Darmstadt, Germany), and 10 mM HEPES (Merck, Darmstadt, Germany) with a pH of 7.4 saturated with carbogen (95% O$_2$/5% CO$_2$).

The Krumdieck tissue slicer was attached to a water bath that cooled the Krebs-Henseleit buffer to 4 °C. Slices were collected and selected based on round and intact morphology. The slices had a weight between 4–6 mg with an estimated thickness of 300 μm. To ensure viability, the slices were collected in ice cold UW cold storage solution.

For the initial aim, part A, PCKS were individually incubated in 12-well plates under the conditions described in Table 1. The control group represents the standard conditions for incubating renal porcine tissue slices [38]. All slices were incubated at 37 °C in an incubator with 80% O$_2$/5% CO$_2$ while shaking at a rate of 90 rpm for 48 h. The culture media with added compounds were refreshed after 24 h.

Table 1. Experimental conditions for part A.

Experimental Group (*n* = 7)	Treatment
Control	Williams Medium E (1X) + GlutaMAX (WME) (Gibco) + 10 uG/mL ciprofloxacin (Fresenius Kabi, France) + 1.2 mG/mL D-(+)-glucose solution (Sigma-Aldrich, UK) + <1% DMSO
Galunisertib	WME + 10 uG/mL ciprofloxacin + 1.2 mG/mL D-(+)-glucose solution + 10 μM galunisertib (Selleckchem, Munich, Germany) in DMSO (<1%)
Doxycycline	WME + 10 uG/mL ciprofloxacin + 1.2 mG/mL D-(+)-glucose solution + <1% DMSO + 113 μM doxycycline (Vibramycin SF 100 mg/5 mL, Pfizer BV, Capelle aan den Ijssel, The Netherlands)

Table 1. *Cont*.

Experimental Group (*n* = 7)	Treatment
Taurine	WME + 10 uG/mL ciprofloxacin + 1.2 mG/mL D-(+)-glucose solution + <1% DMSO + 80 mM taurine (Sigma Aldrich, Darmstadt, Germany) dissolved in WME
Febuxostat	WME + 10 uG/mL ciprofloxacin + 1.2 mG/mL D-(+)-glucose solution + 16 μM febuxostat (Adenuric 80 mg, Menarini, Florence, Italy) dissolved in DMSO (<1%)

2.4. Inducing Fibrosis in PCKS

To further elucidate the antifibrotic effects of galunisertib, part B, we cultured the PCKS in a similar manner to methods described above. HMP was performed using UW cold storage solution instead of UW preservation solution. PKCS were incubated in 12-well plates supplemented with TGF-β1 to promote fibrosis and a treatment group with 10 μM galunisertib to target the induced fibrosis (Table 2).

Table 2. Experimental conditions part B.

Experimental Group (*n* = 3)	Treatment
Control	DMEM/F-12 medium (Gibco, 31331-028) + 10 uG/mL ciprofloxacin + <1% DMSO
TGF-β1	DMEM/F-12 medium + 10 uG/mL ciprofloxacin + 5 ng/mL TGF-β1 (Roche Diagnostics, Almere The Netherlands) + <1% DMSO
TGF-β1 + galunisertib	DMEM/F-12 medium + 10 uG/mL ciprofloxacin + 5 ng/mL TGF-β1 + 10 μM galunisertib in DMSO (<1%)

2.5. Viability Analysis

Viability of the PCKS was evaluated by assessing the adenosine triphosphate (ATP) content as described by de Graaf et al., 2010 [40]. Three slices per timepoint and condition were individually stored in an Eppendorf tube with MiniBeads (Biospec products, Bartlesville, OK, USA) containing 1 mL of sonification solution (70% ethanol and 2 mM EDTA) and snap frozen in liquid nitrogen. A bioluminescence kit was used to measure ATP levels (Roche Diagnostics, Almere, The Netherlands). Luminescence was measured using a luminometer (LumiCountä, Packard, IL, USA). The obtained ATP value was normalized against the total protein content which was measured using a Pierce[TM] BCA protein assay kit. The final ATP content was expressed as pmol ATP/μg protein.

2.6. Gene Expression Analysis

Gene expression for multiple pro-fibrotic genes was assessed with quantitative real-time polymerase chain reaction (PCR). RNA was isolated from five pooled, snap-frozen, precision-cut tissue slices using TRIZOL reagent (Invitrogen, Waltham, MA, USA). Extracted RNA was reverse-transcribed at 70 °C for 10 min, at 37 °C for 50 min, and 15 min at 70 °C. Specific primers were used for PCR analysis (Table 3). The PCR started with 20 s at 95 °C, followed by 40 cycles of 1 s at 95 °C, and 20 s at 60 °C. The plate was measured in the QuantStudio[TM] 7 Flex Real Time PCR System (Applied Biosystems, Waltham, MA, USA). Expression levels were corrected with GAPDH as a reference gene (ΔCt) and compared with a pooled control group (ΔΔCt). Next, the fold induction was calculated and the groups were normalized to the control (control set to 1).

Table 3. Primer sequences.

Gene	Forward Primer Sequence	Reverse Primer Sequence
GAPDH	CCTGCCGTCTGGAGAAACC	CTCGGACGCCTGCTTCA
TGF-b1	GGGAGGGTGTTCATGGTAGGA	AGCTCACCCCAAATTCATCTTC
ACTA2	ACGAAGCCCAAAGCAAAAGA	GTTGGTGATGATGCCGTGTTC
SERPINE1	GCAAGTTCGGGCTCCACTAC	TGCATGCCGTAACCTCCTG
Fibronectin 2	TTAACTGTCTGGCCCGCAATAT	AGGCAATTACCAAAGTCATCTGGA
COL1A2	CAAGAAAGGGCCCAACTGGA	AGGGCCTGGGATACCATCAT
Fibronectin 1	GCACCATCCAACTTGCGTTT	TGTACTCGGTTGCTGGTTCC
SERPINH1	TGCAGTCCATCAACGAGTGG	TGGAATCGCTCATCCCAGTG

2.7. Histological Analysis

Slices fixed in 4% formaldehyde and embedded in paraffin were sectioned at 4μm. An immunohistochemical staining for α-smooth muscle actin (α-SMA) was performed. In short, sections were blocked with 30% H_2O_2 and incubated for 1 h with the α-SMA antibody (Sigma-Aldrich, Darmstadt, Germany), followed by an incubation with a second antibody (Rabbit anti- mouse immunoglobin HRP, #P0260, Dako Agilent, Amstelveen, The Netherlands), and a third antibody (Goat anti-rabbit immunoglobin HRP, # P0448, Dako Agilent), to amplify the signal. A quantity of 1% Normal Swine Serum was added (Dako Agilent). The antibody-antigen complex was visualized by adding diaminobenzidine (DAB) (Merck, Amsterdam, The Netherlands). Counterstaining with hematoxylin and dehydration completed the procedure.

The microscopic images were obtained using the NanoZoomer S360 (Hamamatsu, Hamamatsu, Japan) and the quantification, based on positive pixel count, of α-SMA staining was performed using Aperio ImageScope (Leica Biosystems, Richmond, IL, USA).

2.8. Statistical Analysis

GraphPad Prism 9.0 (GraphPad Software, Boston, MA, USA) was used for creating figures and performing statistical analyses. Values are shown as means with standard deviations. Significant differences were analyzed using one-way ANOVA with a Dunnett's multiple comparisons test. The cut-off for statistical significance was set at $p < 0.05$.

3. Results

3.1. The Effect of Antifibrotic Drugs on DCD-PCKS

We first screened the effects of the different antifibrotic compounds in the absence of TGF-β1. ATP content of the PCKS significantly increased after 48 h incubation compared to baseline demonstrating that ATP production was restored after injury due to cold ischemia and slicing. Furthermore, ATP levels remained stable regardless of the treatment (Figure 1). This indicates that the viability of the PCKS was maintained during culture.

Figure 2 shows that 48 h of incubation led to a significant increase in *ACTA2*, *TGFB1*, and *FN2* expression (baseline compared to the control) indicating that fibrotic processes are already active within these 48 h. Supplementing the PCKS with galunisertib significantly lowered the gene expression of all measured fibrosis markers compared to the control with a *p* value of <0.0001 (Figure 2A–D). Doxycycline significantly lowered the gene expression of *TGFB1*, *FN-2*, and *SERPINE1* with a *p* value of <0.05 (Figure 2B–D). Febuxostat supplementation only significantly decreased mRNA expression of *SERPINE1* ($p < 0.0001$) (Figure 2D). Incubation with taurine did not attenuate any of the measured fibrosis markers. Together, these results show that galunisertib had the strongest antifibrotic effect during 48 h of PCKS incubation.
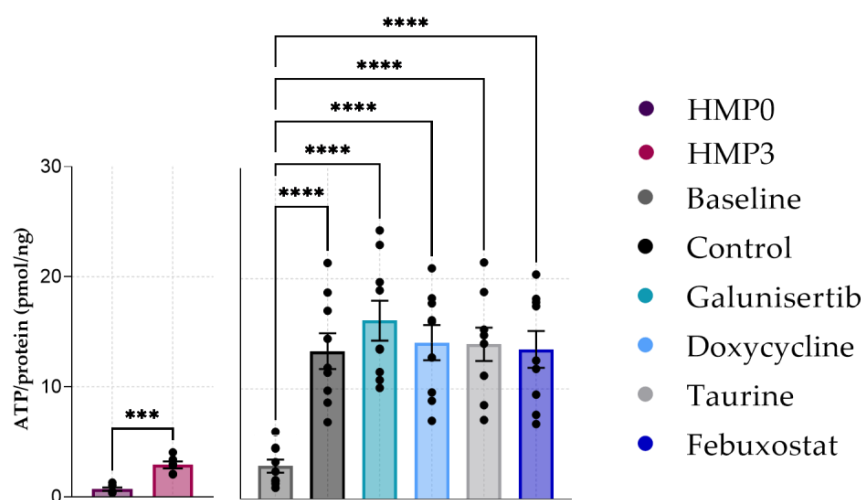
ATP tissue levels

Figure 1. ATP levels in PCKS after 48 h of incubation with antifibrotic treatments. Data shown as individual values and mean ± SEM. *** $p < 0.001$, and **** $p < 0.0001$. The baseline represents slices before incubation. HMP = hypothermic machine perfusion.
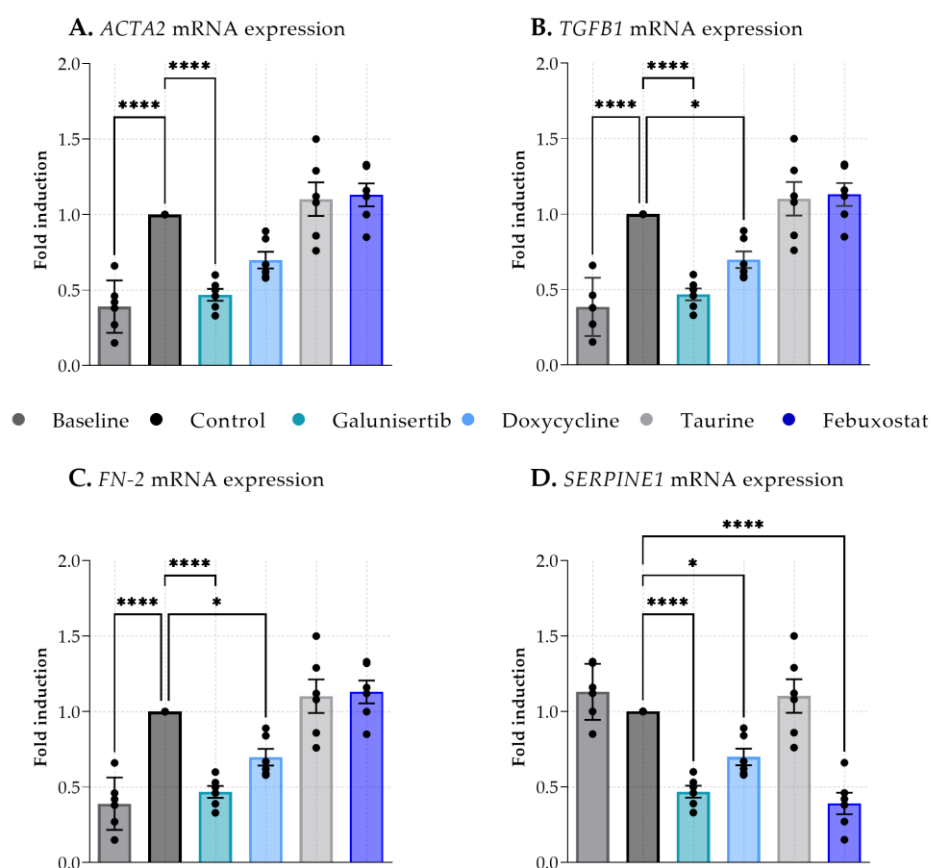

Figure 2. Expression of fibrosis-related genes in kidney cortex tissue of baseline (before incubation) and after 48 h incubation with antifibrotic treatments. (**A**). Actin alpha 2, smooth muscle (*ACTA2*), (**B**). Transforming growth factor beta receptor 1 (*TGFB1*), (**C**). Fibronectin 2 (*FN-2*), (**D**). Serpin family E member 1 (*SERPINE1*). Data shown as individual values and mean ± SEM. Dunnett's multiple comparison was performed by comparing the mean of each group to the mean of the control. * $p < 0.05$; **** $p < 0.0001$.

To observe whether antifibrotic effects were already visible at a protein level, α-SMA levels in tissue were analyzed (Figure 3A). A-SMA levels at baseline were significantly higher compared to the control after 48 h of incubation. The administration of galunisertib, doxycycline taurine or febuxostat did not significantly affect expression of α-SMA compared to the control after 48 h of incubation (Figure 3B).
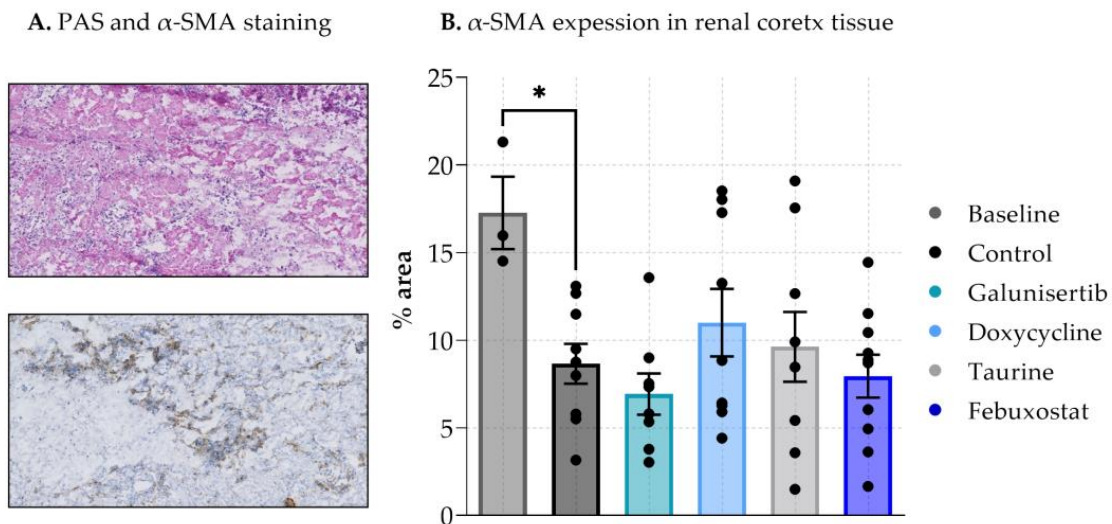
A. PAS and α-SMA staining   **B.** α-SMA expession in renal coretx tissue

Figure 3. Expression of α-SMA in renal cortex tissue after 48 h incubation with antifibrotic treatments. (**A**). shows PAS α-SMA staining on tissue (**B**). shows the expression in % area. Data shown as individual values and mean ± SEM. * $p < 0.05$. The baseline represents slices before incubation.

3.2. The Effect of Galunisertib on Fibrotic PCKS

As galunisertib showed the most significant antifibrotic effects, we then investigated the effects of galunisertib in PCKS that were cultured with TGF-β1 to induce fibrosis. ATP content significantly increased after 48 h compared to baseline (Figure 4). TGF-β1 and the combination of TGF-β1 and galunisertib did not affect ATP content of the PCKS indicating that the viability of the PCKS was maintained during the 48 h of incubation.
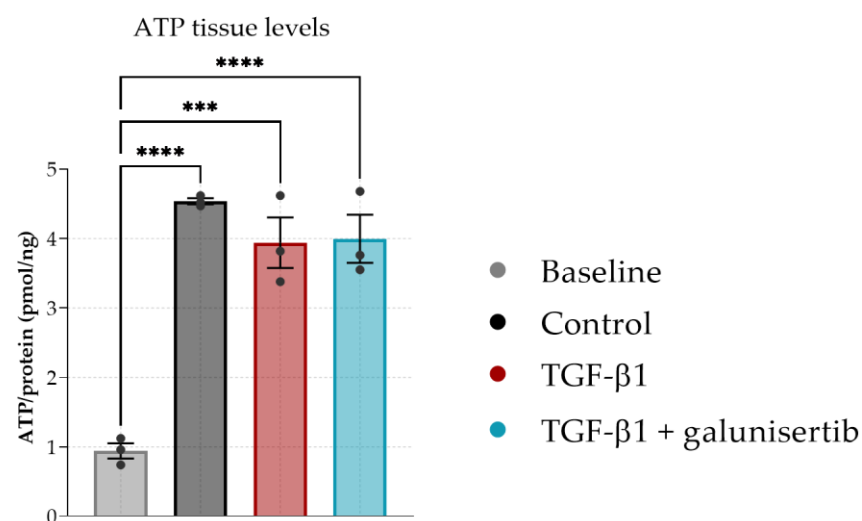

Figure 4. ATP levels in PCKS after 48 h of incubation with TGF-β1 or TGF-β1 and galunisertib. Data shown as individual values and mean ± SEM. Dunnett's multiple comparison was performed by comparing the mean of each group to the mean of the control. *** $p < 0.001$ and **** $p < 0.0001$. The baseline represents slices before incubation.

We then observed the antibiotic effects by analyzing a larger panel of pro-fibrotic markers. Forty-eight hours of incubation led to a significant decrease in *ACTA2* and *SERPINH1* expression (baseline compared to the control) (Figure 5A,E). TGF-β1 promoted fibrosis in PCKS as shown by a significantly increased mRNA expression of *TGFB1*, *FN1*, *SERPINE1*, and *SERPINH1* after 48 h of incubation compared to the control. (Figure 5B–E). Galunisertib, however, clearly attenuated the expression of these pro-fibrotic markers after 48 h of incubation. mRNA expression levels for *ACTA2*, *TGFB1*, *FN1*, *SERPINE1*, *SERPINH1*, and *COL1A2* were significantly lower for tissue slices incubated with galunisertib and TGF-β1 compared to just TGF-β1 (Figure 5A–F). No differences were observed between the control and TGF-β + galunisertib group.
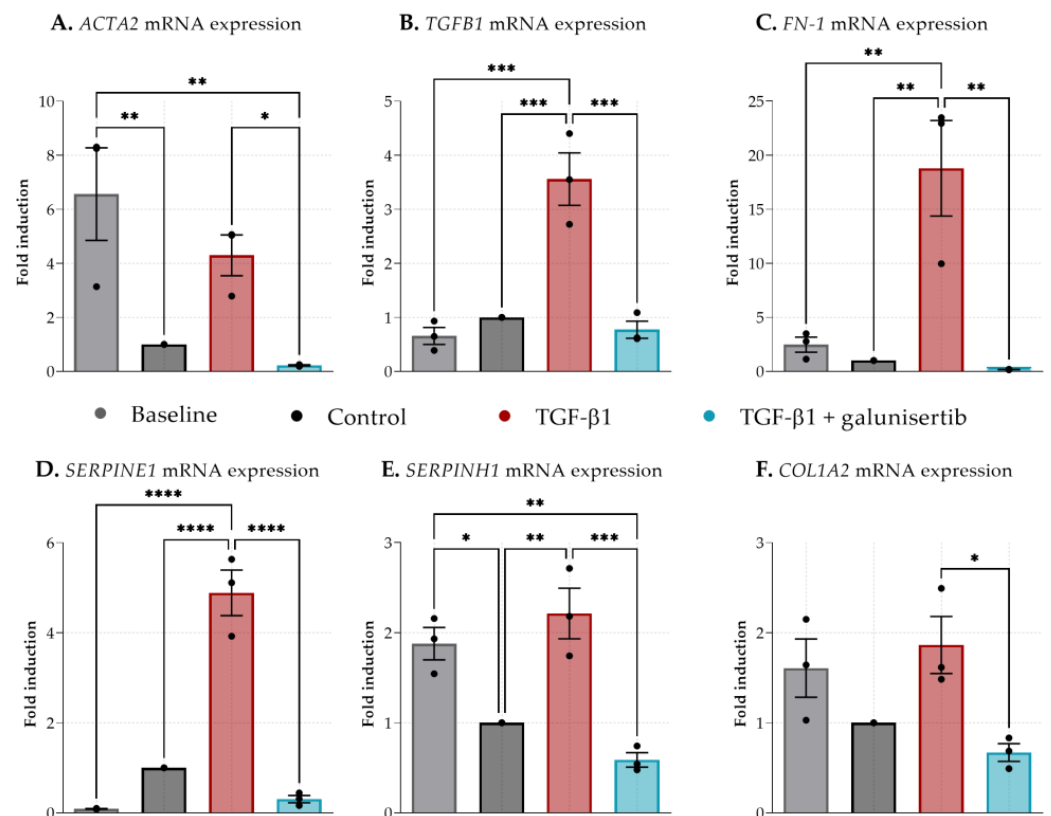

Figure 5. Expression of fibrosis-related genes in kidney cortex tissue after 48 h incubation with TGF-β1 or TGF-β1 and galunisertib. (**A**). Actin alpha 2, smooth muscle (*ACTA2*), (**B**). Transforming growth factor beta receptor 1 (TGFB1), (**C**). Fibronectin 1 (*FN-1*), (**D**). Serpin family E member 1 (*SERPINE1*), (**E**). Serpin Family H Member 1 (*SERPINH1*), and (**F**). Collagen, type I, alpha 2 (*COL1A2*). Data shown as individual values and mean ± SEM. Dunnett's multiple comparison was performed by comparing the mean of each group to the mean of all other groups. * $p < 0.05$; ** $p < 0.01$; *** < 0.001; **** $p < 0.0001$. The baseline represents slices before incubation.

4. Discussion

Interstitial fibrosis formation in DCD renal allografts is a huge burden for the recipient as it leads to loss of renal function, the need for dialysis treatment and/or a re-transplant, and possibly premature death [42,43]. Unfortunately, research into transplant-related renal interstitial fibrosis is lacking due to the availability of proper translational models. Our goal was to assess the antifibrotic potencies of several compounds using porcine DCD-PCKS. This research shows that the combination of machine perfusion and PCKS provide a suitable way to assess antifibrotic pharmaceutical interventions in DCD kidney tissue. Furthermore, we convincingly demonstrated that galunisertib exhibits antifibrotic effects.

Incubation with doxycycline significantly downregulated three of the four measured fibrosis markers. In a previous study, we showed that the addition of doxycycline dur-

ing HMP results in lower NGAL levels [32]. However, we did not see any significant differences when looking at the mRNA expression of fibrosis markers. Moser et al. and Cortes et al. showed similar protective effects of doxycycline in rat kidneys exposed to ischemia-reperfusion injury [31,33].

Taurine did not seem to have any significant antifibrotic effects and febuxostat only on *SERPINE1* mRNA expression, contrary to previous research [25,28]. This could be because of the administered dosage. In previous studies, taurine was administered to whole animals instead of to single tissue slices. The administered dosage is therefore difficult to translate, and a higher dosage might be necessary for PCKS. Furthermore, these previous studies were performed using rats. The progression of fibrosis in rodent models could have a different timeframe compared with the progression of fibrosis in larger species such as pigs or humans.

The variation in fibrosis induction could also lead to variation in fibrosis progression per model. In PCKS, the onset of pro-inflammatory and profibrotic responses can already be observed and targeted within 48 h because of the damage caused by warm ischemia, the mechanical stress of the tissue-slicing process, and cold ischemia. Here, we show that the addition of TGF-β1, a key mediator of fibrosis [13–15], greatly promoted these profibrotic responses by significantly increasing the expression of a broad range of pro-fibrotic markers after only 48 h of incubation. Rodent fibrosis models do not fully mimic the clinical situation as it is often difficult to distinguish whether the given treatment targets the primary renal injury (e.g., ischemia-reperfusion injury, inflammation) causing attenuation of fibrogenesis [37], or actually targets the fibrosis [44]. Moreover, it usually takes weeks for rodents to develop fibrosis.

We selected several fibrosis-related genes corresponding to various processes involved in renal fibrosis. During the onset of fibrosis, TGF-β is one of the most important cytokines involved [13,14]. TGF-β has the ability to activate myofibroblasts that are characterized by de novo expression of α-SMA. These cells then aim to restore tissue integrity by producing and secreting ECM proteins, especially collagens and fibronectins [10]. HSP47—encoded by the gene *SERPINH1*—is a molecular chaperone that is required for collagen synthesis [45]. Additionally, PAI-1—encoded by the gene *SERPINE1*—promotes the accumulation of collagen and fibronectins and thus stimulates excessive tissue scaring [46].

We observed no significant differences in α-SMA formation between treatments. However, 48 h of incubation could be too short a timeframe to see differences on a protein level. We did observe significant differences in mRNA expression. Galunisertib caused a significant decrease in ACTA2 expression, the gene coding for α-SMA, after 48 h of incubation (Figures 2A and 5A). However, mRNA transcription is a much quicker process than protein translation.

As mentioned before, PCKS provide an elegant platform for testing multiple compounds using the same kidney, keeping biological differences minimal. Because of the size of the porcine kidney and the simplicity of the method, hundreds of slices can be produced and used to assess treatments under a variety of conditions (e.g., timepoints, concentrations, compounds) using various analytical techniques, such as qPCR, staining, and western blotting, allowing a close look at mechanisms of action. Porcine kidneys are anatomically similar to human kidneys and therefore provide a suitable model for translational research [47]. Slaughterhouse kidneys are commonly used in research on renal transplant-related questions and with promising results [38,48–53]. Moreover, they spare us the need for using laboratory animals. Bigaeva et al. showed similar results on gene expression when incubating human (fibrotic) PCKS with 10 μM galunisertib [54], indicating that porcine PCKS provide translatable results.

Limitations

We observed differences between the baseline and control ATP and mRNA levels between our two aims. These differences could be due to the different glucose concentrations between UW machine perfusion solution used during HMP of the first aim and UW

cold storage solution used during the second aim. Glucose is an important component for ATP production and different concentrations of glucose have significant impact on cell viability [55,56]. UW cold storage solution lacks glucose explaining the lower baseline ATP levels in the second aim. However, ATP levels for both aims follow the same trend and are still reliable, as each aim contains its own control.

Although PCKS provide a great way of testing multiple compounds while only needing one kidney, it does not provide insights into how compounds will react in full isolated organs. NMP with added interventions would therefore constitute a valuable follow-up experiment, providing a platform to assess the effects of promising treatments such as galunisertib on renal function in a transplant setting [57,58].

5. Conclusions

This study has provided insights into the antifibrotic potential of several drugs. We show that porcine DCD-PCKS provides an important translational model for answering transplant- and fibrosis-related questions. Furthermore, we show that galunisertib demonstrates strong antifibrotic effects, making it a promising antifibrotic compound for further research in a more preclinical model. Ultimately, galunisertib could be implemented during machine perfusion in a clinical setting as a treatment to prevent or to attenuate fibrosis in DCD kidneys.

Author Contributions: Conceptualization, L.L.v.L., M.J.R.R., H.G.D.L. and P.O.; methodology, L.L.v.L. and M.J.R.R.; formal analysis, L.L.v.L. and M.J.R.R.; data curation, L.L.v.L. and M.J.R.R.; writing—original draft preparation, L.L.v.L.; writing—review and editing, L.L.v.L., M.J.R.R., H.G.D.L. and P.O.; visualization, L.L.v.L.; supervision, H.G.D.L. and P.O. All authors have read and agreed to the published version of the manuscript.

References

1. Webster, A.C.; Nagler, E.V.; Morton, R.L.; Masson, P. Chronic Kidney Disease. *Lancet* **2017**, *389*, 1238–1252. [CrossRef] [PubMed]
2. Schaubel, D.; Desmeules, M.; Mao, Y.; Jeffery, J.; Fenton, S. Survival experience among elderly end-stage renal disease patients. A controlled comparison of transplantation and dialysis. *Transplantation* **1995**, *60*, 1389–1394. [CrossRef] [PubMed]
3. Filiopoulos, V.; Boletis, J.N. Renal transplantation with expanded criteria donors: Which is the optimal immunosuppression? *World J. Transplant.* **2016**, *6*, 103. [CrossRef] [PubMed]
4. Saidi, R.F.; Elias, N.; Kawai, T.; Hertl, M.; Farrell, M.L.; Goes, N.; Wong, W.; Hartono, C.; Fishman, J.A.; Kotton, C.N.; et al. Outcome of Kidney Transplantation Using Expanded Criteria Donors and Donation After Cardiac Death Kidneys: Realities and Costs. *Am. J. Transplant.* **2007**, *7*, 2769–2774. [CrossRef] [PubMed]
5. Venkat, K.K.; Eshelman, A.K. The evolving approach to ethical issues in living donor kidney transplantation: A review based on illustrative case vignettes. *Transplant. Rev.* **2014**, *28*, 134–139. [CrossRef]
6. Li, X.; Zhuang, S. Recent advances in renal interstitial fibrosis and tubular atrophy after kidney transplantation. *Fibrogenesis Tissue Repair* **2014**, *7*, 1–11. [CrossRef]
7. Boor, P.; Floege, J. Renal Allograft Fibrosis: Biology and Therapeutic Targets. *Am. J. Transplant.* **2015**, *15*, 863–886. [CrossRef]
8. Cosio, F.G.; Grande, J.P.; Larson, T.S.; Gloor, J.M.; Velosa, J.A.; Textor, S.C.; Griffin, M.D.; Stegall, M.D. Kidney Allograft Fibrosis and Atrophy Early After Living Donor Transplantation. *Am. J. Transplant.* **2005**, *5*, 1130–1136. [CrossRef]
9. Yuan, Q.; Tan, R.J.; Liu, Y. Myofibroblast in Kidney Fibrosis: Origin, Activation, and Regulation. *Ren. Fibros. Mech. Therapies* **2019**, *1165*, 253–283.

10. LeBleu, V.; Taduri, G.; O'Connell, J.; Teng, Y.; Cooke, V.; Woda, C.; Sugimoto, H.; Kalluri, R. Origin and function of myofibroblasts in kidney fibrosis. *Nat. Med.* **2013**, *19*, 1047–1053. [CrossRef]

11. Mackinnon, A.; Forbes, S. Bone marrow contributions to fibrosis. *Biochim. et Biophys. Acta (BBA)-Mol. Basis Dis.* **2013**, *1832*, 955–961. [CrossRef] [PubMed]

12. Yan, J.; Zhang, Z.; Jia, L.; Wang, Y. Role of bone marrow-derived fibroblasts in renal fibrosis. *Front. Physiol.* **2016**, *7*, 61. [CrossRef] [PubMed]

13. Eddy, A.A. Molecular insights into renal interstitial fibrosis. *J. Am. Soc. Nephrol.* **1996**, *7*, 2495–2508. [CrossRef] [PubMed]

14. Eddy, A.A. Overview of the cellular and molecular basis of kidney fibrosis. *Kidney Int. Suppl.* **2014**, *4*, 2–8. [CrossRef]

15. Liu, Y. Renal fibrosis: New insights into the pathogenesis and therapeutics. *Kidney Int.* **2006**, *69*, 213–217. [CrossRef]

16. Zhao, H.; Dong, Y.; Tian, X.; Tan, T.K.; Liu, Z.; Zhao, Y.; Zhang, Y.; Harris, D.C.; Zheng, G. Matrix metalloproteinases contribute to kidney fibrosis in chronic kidney diseases. *World J. Nephrol.* **2013**, *2*, 84–89. [CrossRef]

17. Hijmans, R.S.; Rasmussen, D.G.K.; Yazdani, S.; Navis, G.; van Goor, H.; Karsdal, M.A.; Genovese, F.; van den Born, J. Urinary collagen degradation products as early markers of progressive renal fibrosis. *J. Transl. Med.* **2017**, *15*, 1–11. [CrossRef]

18. Abrass, C.K.; Hansen, K.M.; Patton, B.L. Laminin α4-Null Mutant Mice Develop Chronic Kidney Disease with Persistent Overexpression of Platelet-Derived Growth Factor. *Am. J. Pathol.* **2010**, *176*, 839–849. [CrossRef]

19. Liu, Y. Cellular and molecular mechanisms of renal fibrosis. *Nat. Rev. Nephrol.* **2011**, *7*, 684–696. [CrossRef]

20. Tan, T.K.; Zheng, G.; Hsu, T.T.; Wang, Y.; Lee, V.W.; Tian, X.; Wang, Y.; Cao, Q.; Wang, Y.; Harris, D.C. Macrophage Matrix Metalloproteinase-9 Mediates Epithelial-Mesenchymal Transition in Vitro in Murine Renal Tubular Cells. *Am. J. Pathol.* **2010**, *176*, 1256–1270. [CrossRef]

21. Kui Tan, T.; Zheng, G.; Hsu, T.T.; Ra Lee, S.; Zhang, J.; Zhao, Y.; Tian, X.; Wang, Y.; Min Wang, Y.; Cao, Q.; et al. Matrix metalloproteinase-9 of tubular and macrophage origin contributes to the pathogenesis of renal fibrosis via macrophage recruitment through osteopontin cleavage. *Lab. Investig.* **2013**, *93*, 434–449. [CrossRef] [PubMed]

22. Isaka, Y. Targeting TGF-β Signaling in Kidney Fibrosis. *Int. J. Mol. Sci.* **2018**, *19*, 2532. [CrossRef] [PubMed]

23. Luangmonkong, T.; Suriguga, S.; Bigaeva, E.; Boersema, M.; Oosterhuis, D.; de Jong, K.P.; Schuppan, D.; Mutsaers, H.A.; Olinga, P. Evaluating the antifibrotic potency of galunisertib in a human ex vivo model of liver fibrosis. *Br. J. Pharmacol.* **2017**, *174*, 3107–3117. [CrossRef] [PubMed]

24. Stribos, E.G.; Seelen, M.A.; van Goor, H.; Olinga, P.; Mutsaers, H.A. Murine Precision-Cut Kidney Slices as an ex vivo Model to Evaluate the Role of Transforming Growth Factor-β1 Signaling in the Onset of Renal Fibrosis. *Front. Physiol.* **2017**, *8*, 1026. [CrossRef] [PubMed]

25. Cavdar, Z.A.H.İ.D.E.; Ural, C.; Celik, A.; Arslan, S.; Terzioglu, G.; Ozbal, S.; Yildiz, S.; Ergur, U.B.; Guneli, E.; Camsari, T.; et al. Protective effects of taurine against renal ischemia/reperfusion injury in rats by inhibition of gelatinases, MMP-2 and MMP-9, and p38 mitogen-activated protein kinase signaling. *Biotech. Histochem.* **2017**, *92*, 524–535. [CrossRef]

26. Karbalay-Doust, S.; Noorafshan, A.; Pourshahid, S.M. Taxol and taurine protect the renal tissue of rats after unilateral ureteral obstruction: A stereological survey. *Korean J. Urol.* **2012**, *53*, 360–367. [CrossRef]

27. Sato, S.; Yamate, J.; Saito, T.; Hosokawa, T.; Saito, S.; Kurasaki, M. Protective effect of taurine against renal interstitial fibrosis of rats induced by cisplatin. *Naunyn-Schmiedeberg's Arch. Pharmacol.* **2002**, *365*, 277–283. [CrossRef]

28. Cao, J.; Li, Y.; Peng, Y.; Zhang, Y.; Li, H.; Li, R.; Xia, A. Febuxostat Prevents Renal Interstitial Fibrosis by the Activation of BMP-7 Signaling and Inhibition of USAG-1 Expression in Rats. *Am. J. Nephrol.* **2015**, *42*, 369–378. [CrossRef]

29. Roach, D.M.; Fitridge, R.A.; Laws, P.E.; Millard, S.H.; Varelias, A.; Cowled, P.A. Up-regulation of MMP-2 and MMP-9 Leads to Degradation of Type IV Collagen During Skeletal Muscle Reperfusion Injury; Protection by the MMP Inhibitor, Doxycycline. *Eur. J. Vasc. Endovasc. Surg.* **2002**, *23*, 260–269. [CrossRef]

30. Saglam, F.; Celik, A.; Tayfur, D.; Cavdar, Z.; Yilmaz, O.; Sarioglu, S.; Kolatan, E.; Oktay, G.; Camsari, T. Decrease in cell proliferation by an matrix metalloproteinase inhibitor, doxycycline, in a model of immune-complex nephritis. *Nephrology* **2010**, *15*, 560–567. [CrossRef]

31. Cortes, A.L.; Gonsalez, S.R.; Rioja, L.S.; Oliveira, S.S.; Santos, A.L.; Prieto, M.C.; Melo, P.A.; Lara, L.S. Protective outcomes of low-dose doxycycline on renal function of Wistar rats subjected to acute ischemia/reperfusion injury. *Biochim. et Biophys. Acta (BBA)-Mol. Basis Dis.* **2018**, *1864*, 102–114. [CrossRef]

32. van Leeuwen, L.; Venema, L.H.; Heilig, R.; Leuvenink, H.G.; Kessler, B.M. Doxycycline Alters the Porcine Renal Proteome and Degradome during Hypothermic Machine Perfusion. *Curr. Issues Mol. Biol.* **2022**, *44*, 559–577. [CrossRef] [PubMed]

33. Moser, M.A.; Arcand, S.; Lin, H.B.; Wojnarowicz, C.; Sawicka, J.; Banerjee, T.; Luo, Y.; Beck, G.R.; Luke, P.P.; Sawicki, G. Protection of the Transplant Kidney from Preservation Injury by Inhibition of Matrix Metalloproteinases. *PLoS ONE* **2016**, *11*, e0157508. [CrossRef] [PubMed]

34. Hosgood, S.A.; Nicholson, M.L. First in man renal transplantation after ex vivo normothermic perfusion. *Transplantation* **2011**, *92*, 735–738. [CrossRef] [PubMed]

35. Hosgood, S.A.; Saeb-Parsy, K.; Hamed, M.O.; Nicholson, M.L. Successful Transplantation of Human Kidneys Deemed Untransplantable but Resuscitated by Ex Vivo Normothermic Machine Perfusion. *Am. J. Transplant.* **2016**, *16*, 3282–3285. [CrossRef]

36. Hosgood, S.A.; Thompson, E.; Moore, T.; Wilson, C.H.; Nicholson, M.L. Normothermic machine perfusion for the assessment and transplantation of declined human kidneys from donation after circulatory death donors. *J. Br. Surg.* **2018**, *105*, 388–394. [CrossRef]

37. van Leeuwen, L.L.; Leuvenink, H.G.D.; Olinga, P.; Ruigrok, M.J.R. Shifting paradigms for suppressing fibrosis in kidney transplants: Supplementing perfusion solutions with antifibrotic drugs. *Front. Med.* **2022**, *8*, 2917. [CrossRef]

38. van Furth, L.A.; Leuvenink, H.G.; Seras, L.; de Graaf, I.A.; Olinga, P.; van Leeuwen, L.L. Exploring Porcine Precision-Cut Kidney Slices as a Model for Transplant-Related Ischemia-Reperfusion Injury. *Transplantology* **2022**, *3*, 139–151. [CrossRef]

39. Stribos, E.G.; Luangmonkong, T.; Leliveld, A.M.; De Jong, I.J.; Van Son, W.J.; Hillebrands, J.L.; Seelen, M.A.; Van Goor, H.; Olinga, P.; Mutsaers, H.A. Precision-cut human kidney slices as a model to elucidate the process of renal fibrosis. *Transl. Res.* **2016**, *170*, 8–16. [CrossRef]

40. de Graaf, I.A.; Olinga, P.; de Jager, M.H.; Merema, M.T.; de Kanter, R.; van de Kerkhof, E.G.; Groothuis, G.M. Preparation and incubation of precision-cut liver and intestinal slices for application in drug metabolism and toxicity studies. *Nat. Protoc.* **2010**, *5*, 1540–1551. [CrossRef]

41. Stribos, E.G.; Hillebrands, J.L.; Olinga, P.; Mutsaers, H.A. Renal fibrosis in precision-cut kidney slices. *Eur. J. Pharmacol.* **2016**, *790*, 57–61. [CrossRef] [PubMed]

42. Matas, A.J.; Gillingham, K.J.; Humar, A.; Kandaswamy, R.; Sutherland, D.E.; Payne, W.D.; Dunn, T.B.; Najarian, J.S. 2202 kidney transplant recipients with 10 years of graft function: What happens next? *Am. J. Transplant.* **2008**, *8*, 2410–2419. [CrossRef]

43. Dinis, P.; Nunes, P.; Marconi, L.; Furriel, F.; Parada, B.; Moreira, P.; Figueiredo, A.; Bastos, C.; Roseiro, A.; Dias, V.; et al. Kidney Retransplantation: Removal or Persistence of the Previous Failed Allograft? *Transplant. Proc.* **2014**, *46*, 1730–1734. [CrossRef] [PubMed]

44. Boor, P.; Šebeková, K.; Ostendorf, T.; Floege, J. Treatment targets in renal fibrosis. *Nephrol. Dial. Transplant.* **2007**, *22*, 3391–3407. [CrossRef]

45. Razzaque, M.S.; Le, V.T.; Taguchi, T. Heat Shock Protein 47 and Renal Fibrogenesis. *Cell. Stress Responses Ren. Dis.* **2005**, *148*, 57–69.

46. Ghosh, A.K.; Vaughan, D.E. PAI-1 in Tissue Fibrosis. *J. Cell. Physiol.* **2012**, *227*, 493–507. [CrossRef]

47. Golriz, M.; Fonouni, H.; Nickkholgh, A.; Hafezi, M.; Garoussi, C.; Mehrabi, A. Pig Kidney Transplantation: An Up-To-Date Guideline. *Eur. Surg. Res.* **2012**, *49*, 121–129. [CrossRef]

48. Grosse-Siestrup, C.; Unger, V.; Fehrenberg, C.; Baeyer, H.V.; Fischer, A.; Schäper, F.; Groneberg, D.A. A model of isolated autologously hemoperfused porcine slaughterhouse kidneys. *Nephron* **2002**, *92*, 414–421. [CrossRef]

49. Venema, L.H.; Brat, A.; Moers, C.; A't Hart, N.; Ploeg, R.J.; Hannaert, P.; Minor, T.; Leuvenink, H.G. Effects of Oxygen During Long-term Hypothermic Machine Perfusion in a Porcine Model of Kidney Donation After Circulatory Death. *Transplantation* **2019**, *103*, 2057–2064. [CrossRef]

50. Hendriks, K.D.; Brüggenwirth, I.M.; Maassen, H.; Gerding, A.; Bakker, B.; Porte, R.J.; Henning, R.H.; Leuvenink, H.G. Renal temperature reduction progressively favors mitochondrial ROS production over respiration in hypothermic kidney preservation. *J. Transl. Med.* **2019**, *17*, 1–10. [CrossRef]

51. Pool, M.B.F.; Hartveld, L.; Leuvenink, H.G.D.; Moers, C. Normothermic machine perfusion of ischaemically damaged porcine kidneys with autologous, allogeneic porcine and human red blood cells. *PLoS ONE* **2020**, *15*, e0229566. [CrossRef] [PubMed]

52. Karuthu, S.; Blumberg, E.A. Common infections in kidney transplant recipients. *Clin. J. Am. Soc. Nephrol.* **2012**, *7*, 2058–2070. [CrossRef] [PubMed]

53. Blum, M.F.; Liu, Q.; Soliman, B.; Dreher, P.; Okamoto, T.; Poggio, E.D.; Goldfarb, D.A.; Baldwin III, W.M.; Quintini, C. Comparison of normothermic and hypothermic perfusion in porcine kidneys donated after cardiac death. *J. Surg. Res.* **2017**, *216*, 35–45. [CrossRef] [PubMed]

54. Bigaeva, E. *Ex Vivo Fibrosis Research: 5 MM Closer to Human Studies*; University of Groningen: Groningen, The Netherlands, 2019; pp. 1–301.

55. Bonora, M.; Patergnani, S.; Rimessi, A.; de Marchi, E.; Suski, J.M.; Bononi, A.; Giorgi, C.; Marchi, S.; Missiroli, S.; Poletti, F.; et al. ATP synthesis and storage. *Purinergic Signal* **2012**, *8*, 343–357. [CrossRef]

56. Cisewski, S.E.; Zhang, L.; Kuo, J.; Wright, G.J.; Wu, Y.; Kern, M.J.; Yao, H. The effects of oxygen level and glucose concentration on the metabolism of porcine TMJ disc cells. *Osteoarthr. Cartil.* **2015**, *23*, 1790–1796. [CrossRef]

57. Brat, A.; Pol, R.A.; Leuvenink, H.G.D. Novel preservation methods to increase the quality of older kidneys. *Curr. Opin. Organ Transplant.* **2015**, *20*, 438–443. [CrossRef]

58. Hosgood, S.A.; van Heurn, E.; Nicholson, M.L. Normothermic machine perfusion of the kidney: Better conditioning and repair? *Transpl. Int.* **2015**, *28*, 657–664. [CrossRef]